Article

Cell Reports

Identification of Nucleolus-Associated Chromatin Domains Reveals a Role for the Nucleolus in 3D Organization of the *A. thaliana* Genome

Graphical Abstract

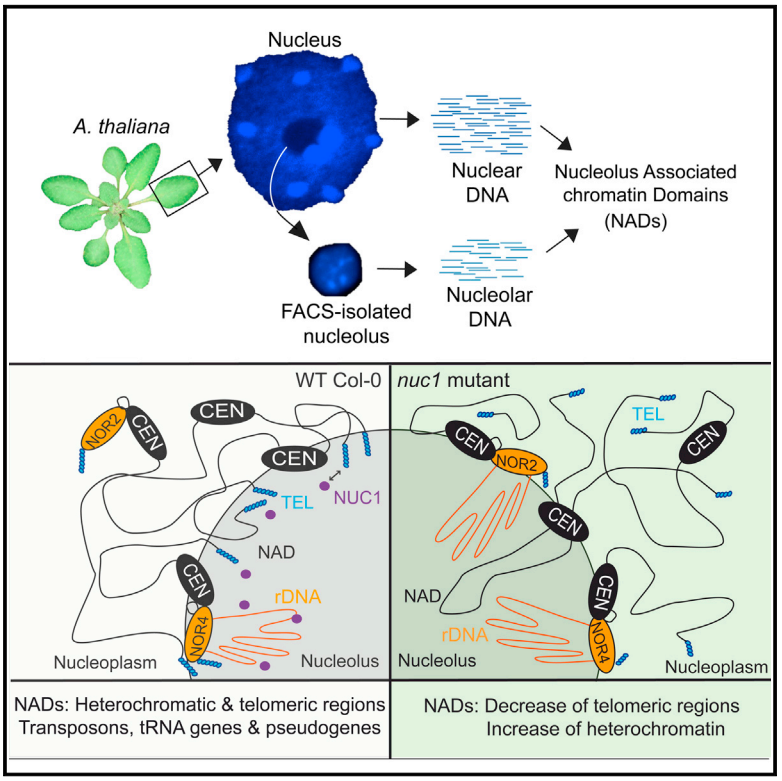

Highlights

- Characterization of nucleolus-associated chromatin domains (NADs) in *A. thaliana*
- Role of the nucleolus and NUC1 in the spatial organization of the genome
- Role of the nucleolus and NUC1 in telomere maintenance

Authors

Frédéric Pontvianne, Marie-Christine Carpentier, Nathalie Durut, ..., Miloslava Fojtová, Jiří Fajkus, Julio Sáez-Vásquez

Correspondence

fpontvia@univ-perp.fr

In Brief

To evaluate the effect of the nucleolus in plant genome organization, Pontvianne et al. identify nucleolus-associated chromatin domains (NADs) in *A. thaliana* leaves. NADs are enriched in regions displaying heterochromatic signatures. We find roles for Nucleolin 1 (NUC1) and the nucleolus in the spatial organization of chromosomes and also in telomere maintenance.

Pontvianne et al., 2016, Cell Reports *16*, 1574–1587
August 9, 2016
http://dx.doi.org/10.1016/j.celrep.2016.07.016

OPEN ACCESS
CellPress

Cell Reports
Article

Identification of Nucleolus-Associated Chromatin Domains Reveals a Role for the Nucleolus in 3D Organization of the *A. thaliana* Genome

Frédéric Pontvianne,[1,2,5,*] Marie-Christine Carpentier,[1,2] Nathalie Durut,[1,2] Veronika Pavlištová,[3] Karin Jaške,[3] Šárka Schořová,[3] Hugues Parrinello,[4] Marine Rohmer,[4] Craig S. Pikaard,[5,6] Miloslava Fojtová,[3] Jiří Fajkus,[3,7] and Julio Sáez-Vásquez[1,2,7]

[1]CNRS, Laboratoire Génome et Développement des Plantes, UMR5096, 66860 Perpignan, France
[2]Université de Perpignan Via Domitia, Laboratoire Génome et Développement des Plantes, UMR5096, 66860 Perpignan, France
[3]Central European Institute of Technology and Faculty of Science, Masaryk University, 62500 Brno, Czech Republic
[4]Montpellier GenomiX, Montpellier Cedex 5, France
[5]Department of Biology and Department of Molecular and Cellular Biochemistry, Indiana University, Bloomington, IN 47405, USA
[6]Howard Hughes Medical Institute, Indiana University, Bloomington, IN 47405, USA
[7]Co-senior author
*Correspondence: fpontvia@univ-perp.fr
http://dx.doi.org/10.1016/j.celrep.2016.07.016

SUMMARY

The nucleolus is the site of rRNA gene transcription, rRNA processing, and ribosome biogenesis. However, the nucleolus also plays additional roles in the cell. We isolated nucleoli using fluorescence-activated cell sorting (FACS) and identified nucleolus-associated chromatin domains (NADs) by deep sequencing, comparing wild-type plants and null mutants for the nucleolar protein NUCLEOLIN 1 (NUC1). NADs are primarily genomic regions with heterochromatic signatures and include transposable elements (TEs), sub-telomeric regions, and mostly inactive protein-coding genes. However, NADs also include active rRNA genes and the entire short arm of chromosome 4 adjacent to them. In *nuc1* null mutants, which alter rRNA gene expression and overall nucleolar structure, NADs are altered, telomere association with the nucleolus is decreased, and telomeres become shorter. Collectively, our studies reveal roles for NUC1 and the nucleolus in the spatial organization of chromosomes as well as telomere maintenance.

INTRODUCTION

An important aspect of transcriptional regulation is the modification of gene accessibility to transcription factors and RNA polymerases. Gene accessibility depends on local chromatin structure but also on the nuclear context and subnuclear localization of a gene. In recent years, local chromatin structure and its effect on gene expression has been extensively studied, with genome-wide approaches defining the chromatin contexts for each gene (Filion et al., 2010; Kharchenko et al., 2011; Roudier et al., 2011; Roy et al., 2010; Wang et al., 2008) and identifying chromatin states that correlate with gene activity (Bickmore and van Steensel, 2013; Sequeira-Mendes and Gutierrez, 2015). However, nuclear context is also important in that the position of a gene with respect to nuclear pores, the nuclear lamina, or the nucleolus as well as its inter- or intrachromosome interactions with other loci can affect its transcriptional regulation (Bickmore and van Steensel, 2013).

In mammalian cells, large portions of the genome associate with the nuclear lamina at the periphery of the nucleus and are identified as lamina-associated domains (LADs). LADs are essentially composed of regions with silent chromatin signatures and can represent up to 35% of the nuclear genome (Guelen et al., 2008). Chromosome regions can also associate with the nucleolus, the largest nuclear body. The nucleolus forms as a direct consequence of ribosome biogenesis, but it is also implicated in stress sensing, cell-cycle progression, viral replication, and ribonucleoprotein (RNP) biogenesis (Boisvert et al., 2007; Boulon et al., 2010; Pederson, 2011). Nucleolus-associated chromatin domains (NADs) represent several megabases of the human genome from all 23 chromosomes, typically regions displaying silent chromatin signatures (Németh et al., 2010; van Koningsbruggen et al., 2010). Comparison of NADs and LADs has revealed substantial overlap. Interestingly, LADs that do not relocate to the nuclear periphery after mitosis often associate instead with the nucleolus (Kind et al., 2013, 2015). An important aspect of the nucleolus is that it creates a large domain within the nucleus from which RNA polymerase II (RNA Pol II) is absent (Schubert and Weisshart, 2015). There is no membrane or physical barrier separating the nucleolus from the nucleoplasm, suggesting that nucleolar chromatin bears modifications that are refractory to Pol II transcription. Indeed, mutations in chromatin modifiers that localize and act (in part) in the nucleolus, such as *Arabidopsis* HISTONE DEACETYLASE 6, result in Pol II detection in the nucleolus as well as Pol II association with rRNA genes, which are usually transcribed only by Pol I (Earley et al., 2010). In plant cells, neither LADs nor NADs have been identified so far. Importantly, plants lack genes orthologous to those encoding nuclear lamins in other eukaryotes. However,

little nuclei (LINC) (also called CRWN) proteins share some characteristics with lamins, including coiled-coil domains (Dittmer et al., 2007). However, an association between this complex and chromatin has not yet been demonstrated.

The relationship between rRNA gene transcription and organization and the nucleolus has been studied extensively (Benoit et al., 2013; Grummt and Längst, 2013; McStay and Grummt, 2008; Tucker et al., 2010). In each cell, active and inactive rRNA genes coexist, and their ratio varies depending on the needs of the cell. Most silent copies of rRNA genes are excluded from the nucleolus, where RNA polymerase I is located, but they relocate into the nucleolus in mutants that disrupt silencing (Pontvianne et al., 2013).

rRNA genes are arranged in tandem arrays (known as nucleolus organizer regions [NORs]) that span millions of base pairs. Because silenced rRNA genes comprise a NOR on a different chromosome from active rRNA genes in *Arabidopsis thaliana* (ecotype Col-0), changes in rRNA gene activity that are accompanied by changes in their subnuclear localization (Pontvianne et al., 2013) are predicted to affect chromosome organization within the nucleus, at least locally. Using a technique that allows us to isolate nucleoli from plant tissue using fluorescence-activated cell sorting (FACS) combined with deep sequencing, we now report the identification of genomic NADs in the cell nuclei of *A. thaliana* leaves. We show that NADs other than rRNA genes are mainly composed of transposable elements (TEs) but that NADs also contain genes that are weakly expressed or unexpressed. Analyses of NADs in the *nucleolin 1* (*nuc1*) mutant, which disrupts rRNA gene silencing at the inactive NOR and alters nucleolar structure, reveals that NAD composition changes in *nuc1* versus wild-type nuclei. Interestingly, *nuc1* mutants also display shortened telomeres, and telomerase activity is detected in immunoprecipitated NUC1 fractions, revealing an effect linking the nucleolar protein NUC1 with telomere maintenance.

RESULTS

Identification of NADs in *A. thaliana*

DNA staining using the fluorescent dye DAPI allows the visualization of nuclear DNA and its distribution within the nucleus. In nuclei of 3-week-old *A. thaliana* leaves, bright DAPI-intensive signals correspond to chromocenters that include the highly compacted peri-centromeric heterochromatin of the ten chromosomes. On the other hand, euchromatin is less compact, and therefore the DAPI signal is less intense. DAPI staining of nuclei also allows one to identify the nucleolus, which appears as a black cavity in the nucleus because of a 3-fold lower concentration of DNA in the nucleolus compared with the surrounding nucleoplasm (excluding centromeres) (Figure 1A; see fluorescence intensity plot). To characterize this nucleolar DNA, we took advantage of a method that we recently developed for the purification of nucleoli by a modified FACS approach. In this protocol, a nucleolar protein, Fibrillarin, is fused to yellow fluorescent protein (FIB2:YFP) and stably expressed in wild-type Col-0 plants to specifically mark nucleoli (Figure 1A; Pontvianne et al., 2013). Nucleoli liberated from sonicated nuclei are then isolated by fluorescence-activated nucleolar sorting (FANoS). Purified, sorted nucleoli stained by DAPI allow detection of nucleolar DNA (Figure 1B). As in the nucleoplasm, nucleolar DNA is not homogeneously distributed in the nucleolus, and thus stronger DAPI-stained signals are visible in some regions. Because the nucleolus forms around actively transcribed rRNA genes, rRNA genes are detected in nucleolar DNA, as expected, using DNA fluorescence in situ hybridization (FISH) and a probe flanking the transcription initiation site of rRNA genes (Figure 1B; see 45S rDNA signals). Interestingly, rDNA FISH signals do not completely overlap with DAPI-stained nucleolar DNA, suggesting that nucleolar DNA does not consist solely of rRNA genes.

To determine the sequence of nucleolar DNA, two samples consisting of 10^6 nucleoli and two samples of 5×10^5 nuclei from 3-week-old plant leaves were isolated. The nuclear or nucleolar DNA was then purified and sequenced, and reads were mapped to the *Arabidopsis* TAIR10 reference genome. To identify genomic regions present in the nucleolus, we compared read densities of nuclear or nucleolar DNA for each of the two replicates. The nuclear fraction served as an input control to evaluate the relative enrichment of genomic regions in the nucleolar DNA. Genomic regions with a nucleolar versus nuclear (No/N) fold enrichment ratio greater than 2 in both replicates were considered NADs (Figure 1C). Excluding rRNA genes, NADs represent 4.2% of the genome (~5.7 Mb). Around 30% of NADs correspond to genes, 35% correspond to TEs, and the rest correspond to intergenic regions (Figure 1D).

The No/N fold enrichment ratio was plotted along each of the five chromosomes in 100-kb windows to scan for genomic regions associated with the nucleolus (Figure 1E). In *A. thaliana*, 45S rRNA genes are arranged in tandem repeat arrays in NORs located on the left arms of chromosomes 2 and 4 (Figure 1E, *NOR2* and *NOR4*). In *A. thaliana* leaves, only *NOR4* associates with the nucleolus and is actively transcribed, whereas *NOR2* is inactive and is excluded from the nucleolus (Chandrasekhara et al., 2016; Fransz et al., 2002; Pontvianne et al., 2013). This genomic configuration and selective expression of 45S rRNA genes is reflected in the enrichment of NADs along the left arm of chromosome 4 and their near absence from the left arm of chromosome 2 (Figure 1E). In fact, the entire left arm of chromosome 4 (or Chr4S for "chromosome 4 short arm"), including its pericentromeric and centromeric regions, associates with the nucleolus (Figure 1E). In contrast, the left arm of chromosome 2 behaves like chromosomes 1, 3, and 5, which do not harbor NORs. Subtelomeric regions from all five chromosome pairs are also enriched in the nucleolus, consistent with previous work demonstrating telomere clustering at the periphery of the nucleolus (Armstrong et al., 2001).

NADs Are Enriched in Inactive Chromatin Marks and TEs

We took advantage of published epigenomic data to characterize the types of chromatin that associate with NADs. Among the nine chromatin states defined based on their histone marks and histone variant content (Sequeira-Mendes et al., 2014), and presented in Figure S1A, we found that four were statistically

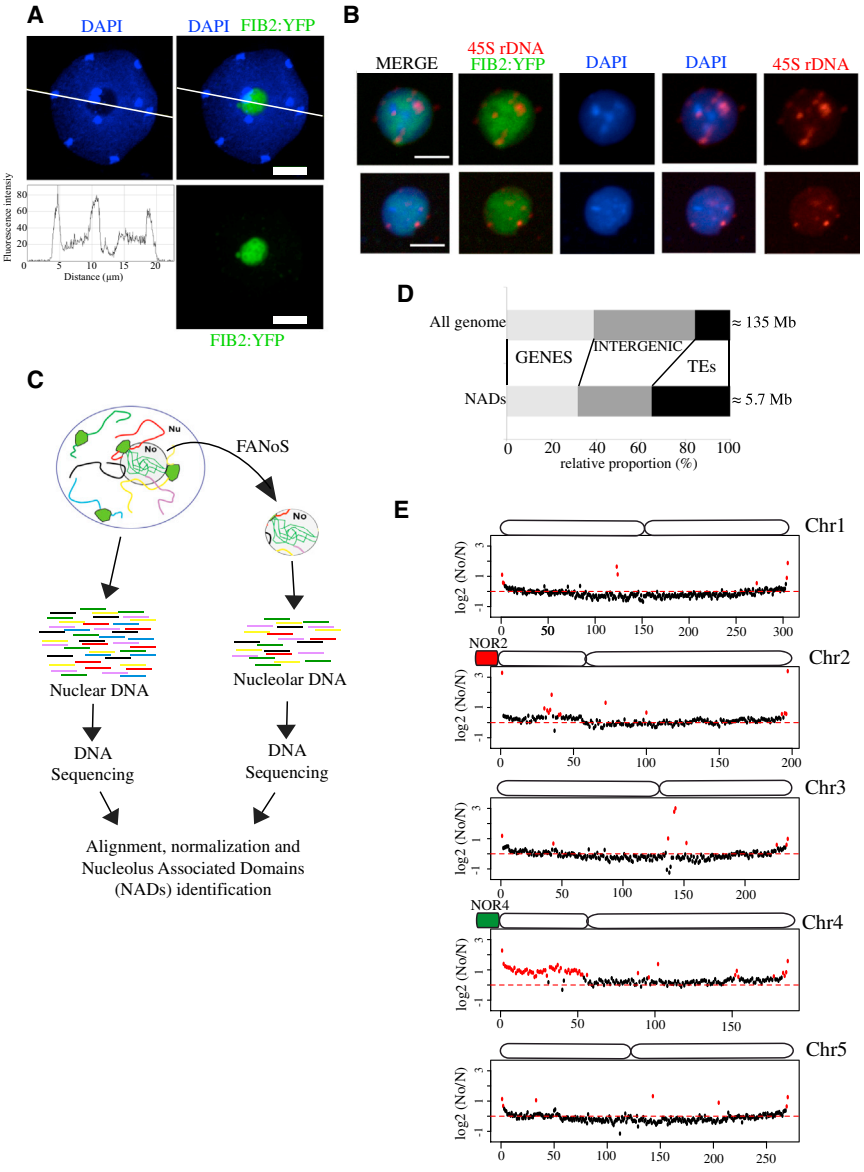

Figure 1. Identification of NADs in *A. thaliana*

(A) One z stack of a DAPI-stained (blue) nucleus from an *A. thaliana* leaf expressing the Fib2:YFP (green) marker. The white line segment indicates positions traversing the nucleus where DAPI signal intensity was plotted as a function of distance along the segment (profile below). Scale bars, 5 μm.

(B) Confocal images of two FACS-isolated nucleoli where DNA is stained by DAPI (blue), the Fib2:YFP marker delimits the nucleolus (green), and rRNA genes are detected by DNA FISH (rDNA, red). Scale bars, 2 μm.

(C) Cartoon depicting the strategy used to isolate and sequence total nuclear (Nu) and specifically nucleolar (No) DNA to identify NADs by deep sequencing.

(D) Bar plot displaying the proportion of different types of sequences in NADs (bottom) relative to the entire genome (top).

(E) Chromosome plots displaying the relative enrichment of a given genomic segment in the nucleolus of wild-type Col-0. The y axis displays the fold change ratio No/N. Each dot represents a 100-kb window. Nucleolus-enriched genomic regions above the threshold (red dotted line) are shown in red.

enriched in NADs (Figure 2A). This includes chromatin states 8 and 9, which show an enrichment for CG methylation, and for the silent chromatin marks histone H3 lysine 9 dimethylation and histone H3 lysine 27 monomethylation (H3K9me2 and H3K27me1, respectively) (Sequeira-Mendes et al., 2014). Chromatin states 8 and 9 are typically associated with TEs and intergenic regions. In addition, chromatin states 4 and 5, which are characterized by high levels of H3 lysine 27 trimethylation (H3K27me3), are also enriched in NADs. Although almost no genes (other than TEs) are present in chromatin states 8 and 9, some are present in chromatin states 4 and 5. We therefore analyzed the relative expression of polyA+ RNA from NAD genes in these different chromatin states to establish a possible correlation between NADs and gene expression (Durut et al., 2014). All four of the chromatin states that are enriched in NADs (4, 5, 8, and 9) correspond to genomic regions depleted in actively transcribed genes (Figures 2B and S1B; Sequeira-Mendes et al., 2014).

Because NADs are enriched in TEs, we examined the relative contribution of each TE superfamily to NADs. 3,640 TEs were identified with a No/N fold enrichment ratio greater than 2 (NAD-TEs, Data S1). In general, no TE superfamily is particularly enriched (Figure 2C). *DNA/Mariner*, *DNA/Pogo*, *DNA/Tc1*, and *pseudo-LINE* elements are slightly overrepresented, whereas *LTR/Copia* or *SINE* superfamilies are underrepresented. The biased presence of particular TE superfamilies in NADs is probably a consequence of their relative abundance in peri-centromeric or knob regions (Figure 2D).

Description of the Genes Present in NADs

Although a large portion of NAD loci correspond to TEs, there are also many genes. Using the Araport11 annotation database and excluding 317 Araport11-referenced TEs and rRNA genes, a total of 907 genes were identified as NAD genes, which represent around 3% of all genes (Data S2). The relative position of NAD genes along all five chromosomes follows the general distribution of NADs, being enriched in subtelomeric regions and in the short arm of chromosome 4 (Figure 3A). NAD gene distribution among eukaryotic orthologous groups of proteins (KOG) revealed that most types of KOGs are represented among NAD genes, with only a slight enrichment for the "cell mobility" category. However, only 21 genes belong to this particular category,

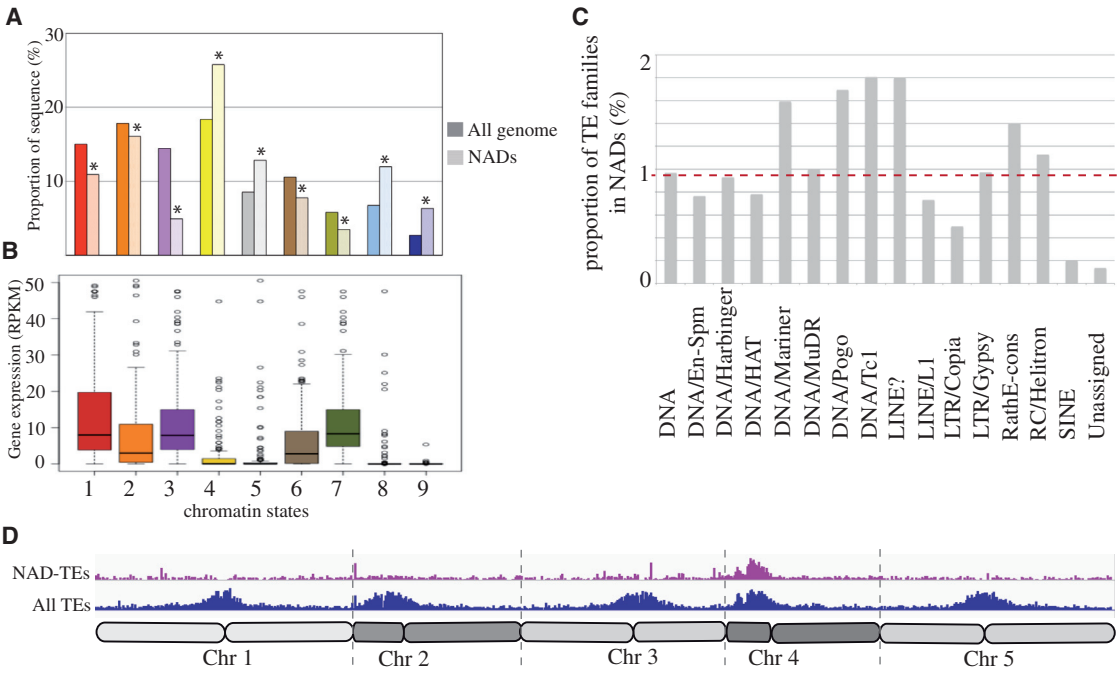

Figure 2. Epigenetic Characteristics of NADs

(A) Histogram representing the relative enrichment of each chromatin state in NADs compared with the entire reference genome.

(B) Box plot representing the relative expression of NAD genes present in each category of the chromatin state. RPKM, reads per kb per million mapped reads.

(C) Histogram displaying the relative proportions of each TE superfamily in NADs. The red dotted line represents the 1× expected enrichment.

(D) Distribution of all TEs (blue) and NAD TEs (violet) along all five chromosomes.

and the 4.7% proportion observed here is only due to the association of one gene and is therefore not considered significant. Genes implicated in "translation, ribosomal structure, and biogenesis," and which are thus linked to nucleolar function, are not enriched among NAD genes either. However, two other categories of genes are particularly enriched: pseudogenes and tRNA genes (Figure 3B). Among the 915 pseudogenes referenced in the *A. thaliana* genome, 72 (7.9%) are present in NAD genes. Moreover, 7.2% of tRNA genes belong to NADs. Interestingly, almost all tRNA isoacceptor types are present in NADs, with the exception of tRNA-His, which is the smallest tRNA gene family in *A. thaliana* (Figure 3D). The global distribution of pre-tRNA genes among the ten chromosome arms shows that 31% are clustered on the short arm of chromosome 2 (Figure S2). Because RNA pol II is not observed in the nucleolus, we expected that predicted pol II-transcribed genes that are among NAD genes would likely be unexpressed or expressed at low levels. Global nuclear gene and NAD gene expression analyses did indeed reveal a bias in expression that supports this hypothesis (Figure 3C).

Effect of NOR Positioning and Nucleolus Structure on NAD Composition

In wild-type *A. thaliana* leaves, only *NOR4* interacts with the nucleolus, whereas *NOR2*, composed of inactive rRNA genes, is excluded from the nucleolar periphery. In null mutants for the *NUCLEOLIN 1* gene (*nuc1*), *NOR2* and *NOR4* both associate with the nucleolus, and the *NOR2* rRNA genes that are normally silenced during development in wild-type leaves fail to silence (Earley et al., 2010; Pontvianne et al., 2010). *VAR1* designates a class of rRNA genes that represent 50% of the entire set of rRNA genes. Because *VAR1* rRNA genes are present at the inactive *NOR2*, they are excluded from the nucleolus, which explains the lack of *VAR1* gene expression in wild-type Col-0 (Chandrasekhara et al., 2016; Pontvianne et al., 2010). However, we previously demonstrated that *VAR1* rRNA genes are expressed in *nuc1* mutants (Pontvianne et al., 2010). Here we show that *VAR1* rRNA genes indeed associate with the nucleolus in the *nuc1* mutant by using PCR analyses of FACS-isolated nuclear or nucleolar DNA (Figure 4A). To test the effect of *NOR2* association with the nucleolus on NAD composition, we isolated and sequenced the DNA from FACS-isolated nuclei or nucleoli of *nuc1*. In wild-type Col-0, chromosome 4 harbors the largest proportion of NADs because of the association of Chr4S with the nucleolus, followed by chromosome 2 (Figure 1). However, in *nuc1*, the short arms of both chromosomes 2 and 4 (Chr2S and Chr4S) associate with the nucleolus (Figure 4B). This observation correlates with the transcriptionally active state of both *NOR2* and *NOR4* in *nuc1* (Figure 4A).

The pericentromeric and centromeric regions of chromosomes 1, 3, and 5 become enriched in *nuc1* mutant NADs (Figures 4C and S3). However, Modullo, the *Drosophila melanogaster* homolog of nucleolin, is required for centromere sequestration at the periphery of the nucleolus (Padeken et al., 2013) so that centromere association with *Arabidopsis* nucleoli might be expected to decrease rather than increase in *nuc1*

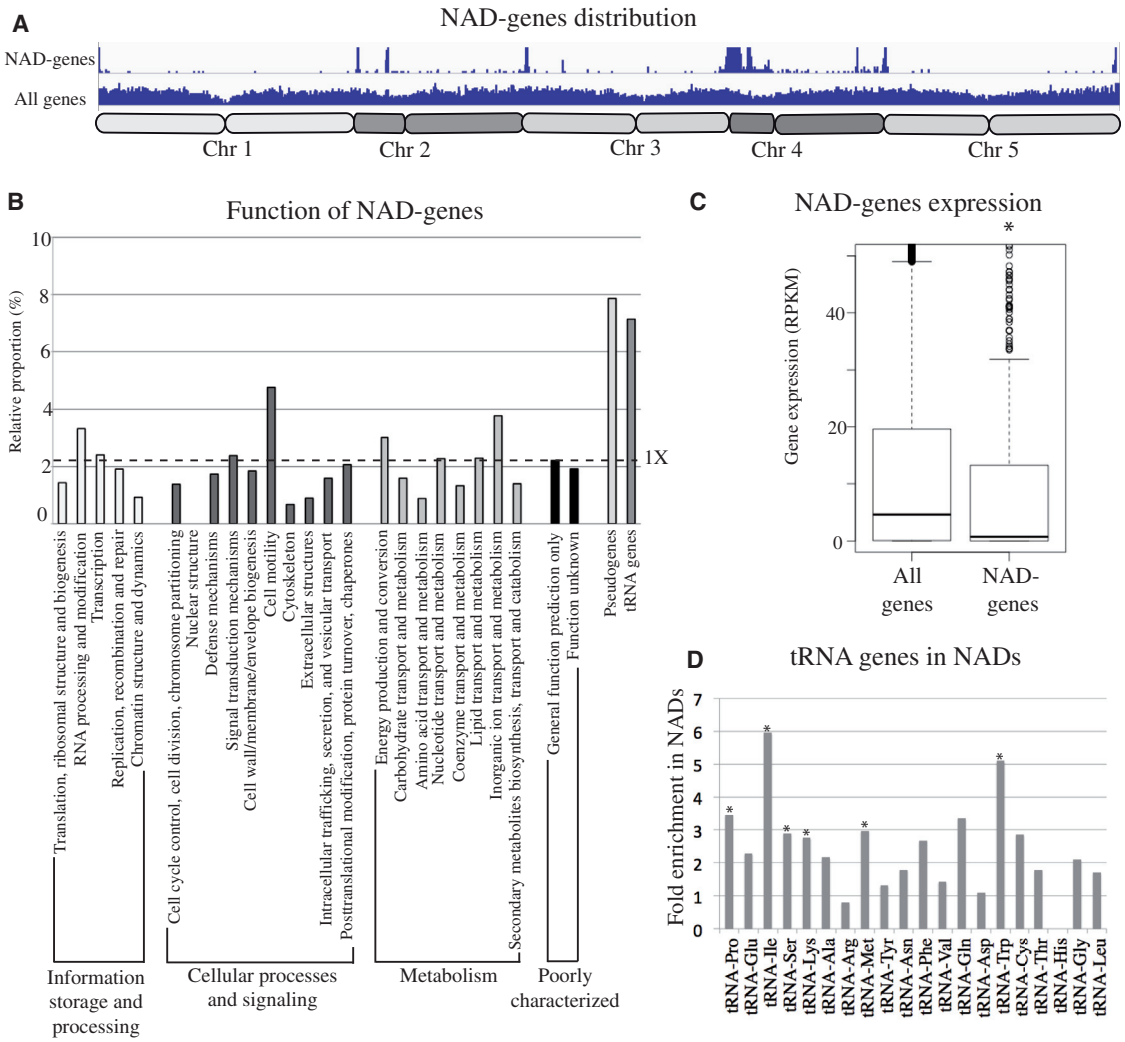

Figure 3. Description of NAD Genes

(A) Distribution of all genes and NAD genes along all five chromosomes.

(B) Histogram displaying the relative enrichment of NAD genes in each cluster of orthologous groups (COGs) among pseudogenes and tRNA genes. The dotted line represents the 1× expected enrichment.

(C) Dot plot revealing the relative expression of all genes or NAD genes in 3-week-old leaves.

(D) Histogram displaying the relative enrichment of each class of tRNA genes in NADs. An asterisk indicates that the enrichment is statistically demonstrated.

mutants. Because centromeric chromocenters are easily detected by DAPI staining, we assessed their relative positions with respect to the nucleolus in wild-type Col-0 and in *nuc1* mutant nuclei from 3-week-old leaves (Figure 4D). In addition, immunolocalization using an antibody recognizing the centromeric Histone 3 (cenH3) were used to validate centromere distribution. Consistent with the NAD analyses, centromeres associate more strongly with the nucleolus in *nuc1* relative to wild-type ($p < 2.2e{-}16$) (Figure 4D). In 16% of the nuclei, a strong DAPI-stained signal can be detected inside Col-0 nucleoli; by contrast, more than 72% of *nuc1* nucleoli harbor these heterochromatin signatures ($p < 2.2e{-}16$) (Figure 4D). The altered centromere positioning in *nuc1* mutant nuclei suggests, as in *D. melanogaster*, a role for NUC1 in heterochromatin distribution but in an opposing way.

NAD Gene Depletion in the *nuc1* Mutant

822 NAD TEs (Data S3) and 117 NAD genes (Data S4) can be identified in *nuc1* with a No/N fold enrichment ratio greater than 2. Their distribution along the five chromosomes (Figure 5A) is quite different from that seen in wild-type Col-0 (Figure 3A). Although 65% of Col-0 NAD genes were distributed on chromosome 4, only 20% of *nuc1* NAD genes are present on this chromosome. By contrast, 13% of Col-0 NAD genes were found on chromosome 2, but this proportion increased to 46% in the *nuc1* mutant. Nonetheless, the NAD gene pool between wild-type Col-0 and *nuc1* overlaps significantly because 80% of *nuc1* NAD genes are also NAD genes in Col-0 (Figure 5B). To further characterize NAD genes that strongly associate with the nucleolus, we identified NAD genes in either wild-type Col-0 or *nuc1* that have an No/N fold enrichment ratio greater than 3

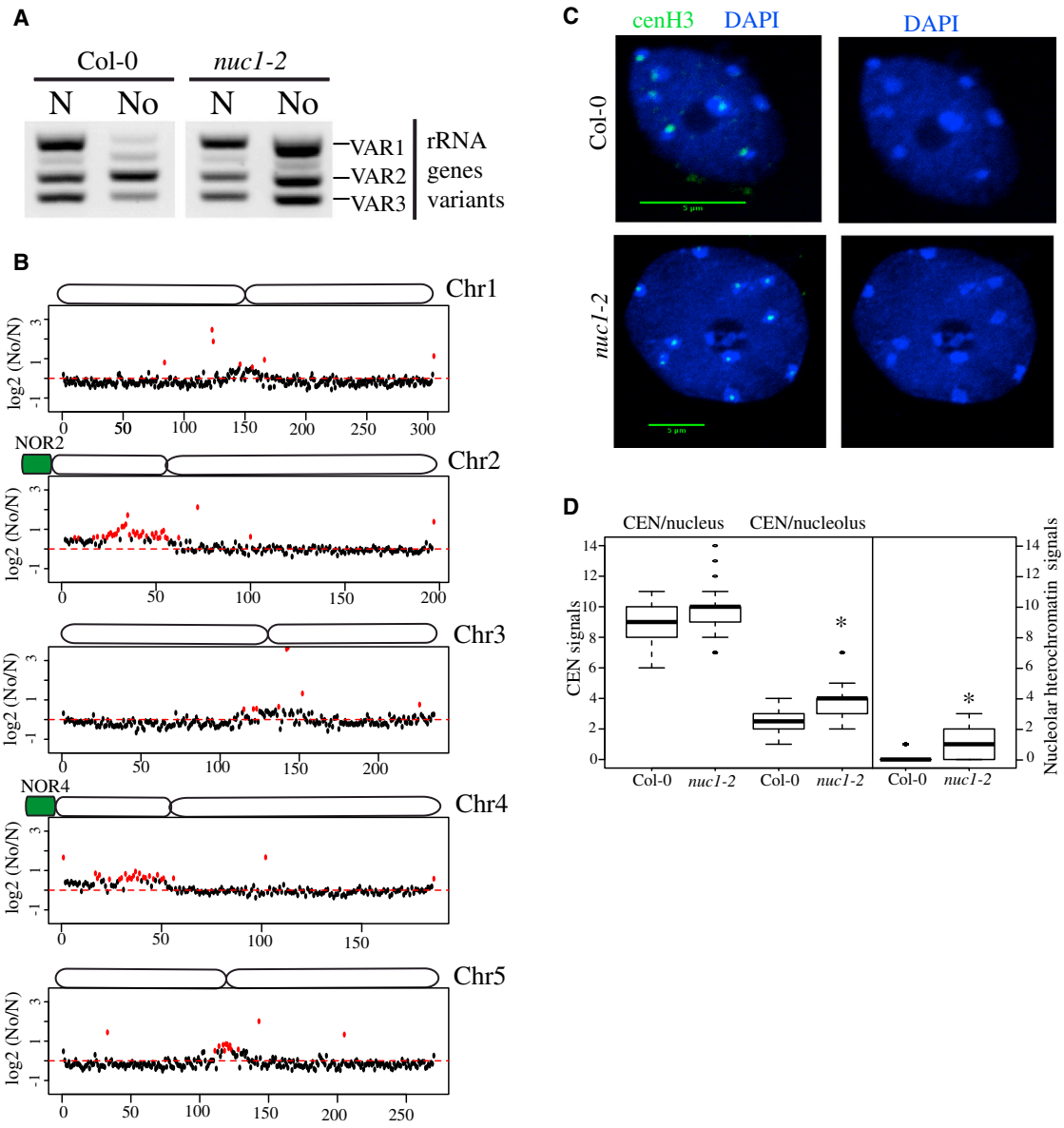

Figure 4. Identification of NADs in the *nuc1* Mutant

(A) PCR detection of rRNA gene variant types in DNA of purified nuclei (N) or nucleoli (No) of wild-type (Col-0) or *nuc1* plants.

(B) Chromosome plots displaying the relative enrichment of the genomic sequence as 100-kb windows in the nucleolus on each five chromosomes in the *nuc1* mutant.

(C) DAPI-stained nuclei from WT Col-0 (left) or from *nuc1* plants (right). The green signal represents the fluorescence obtained from the anti-cenH3 antibody. Scale bars, 5μm.

(D) Box plot showing the relative proportion of nucleolus-associated centromeres (CEN) in WT Col-0 or the *nuc1* mutant. The analysis was performed on 100 nuclei/sample.

(Figure 5C). In both cases, about 100 NAD genes were identified, and 51 were shared in both genotypes. Among these common loci are tRNA genes (8) and pseudogenes (21), demonstrating their strong, reproducible association with the nucleolus, even in the *nuc1* mutant context, where nucleolar structure is disrupted (Pontvianne et al., 2007).

Because RNA pol II is generally not detected in the nucleolus, we hypothesized that the physical association of NAD genes with the nucleolus may reflect their transcriptional status. We thus took advantage of the fact that several hundred NAD genes detected in the wild-type no longer associate with the nucleolus in the *nuc1* mutant to see whether loss of nucleolar localization correlates with their activity. RNA deep sequencing analyses of Col-0 versus the *nuc1* mutant from 3-week-old leaves were performed in triplicate, allowing us to identify 100 upregulated genes in the *nuc1* mutant (Figure 5C). Among these 100

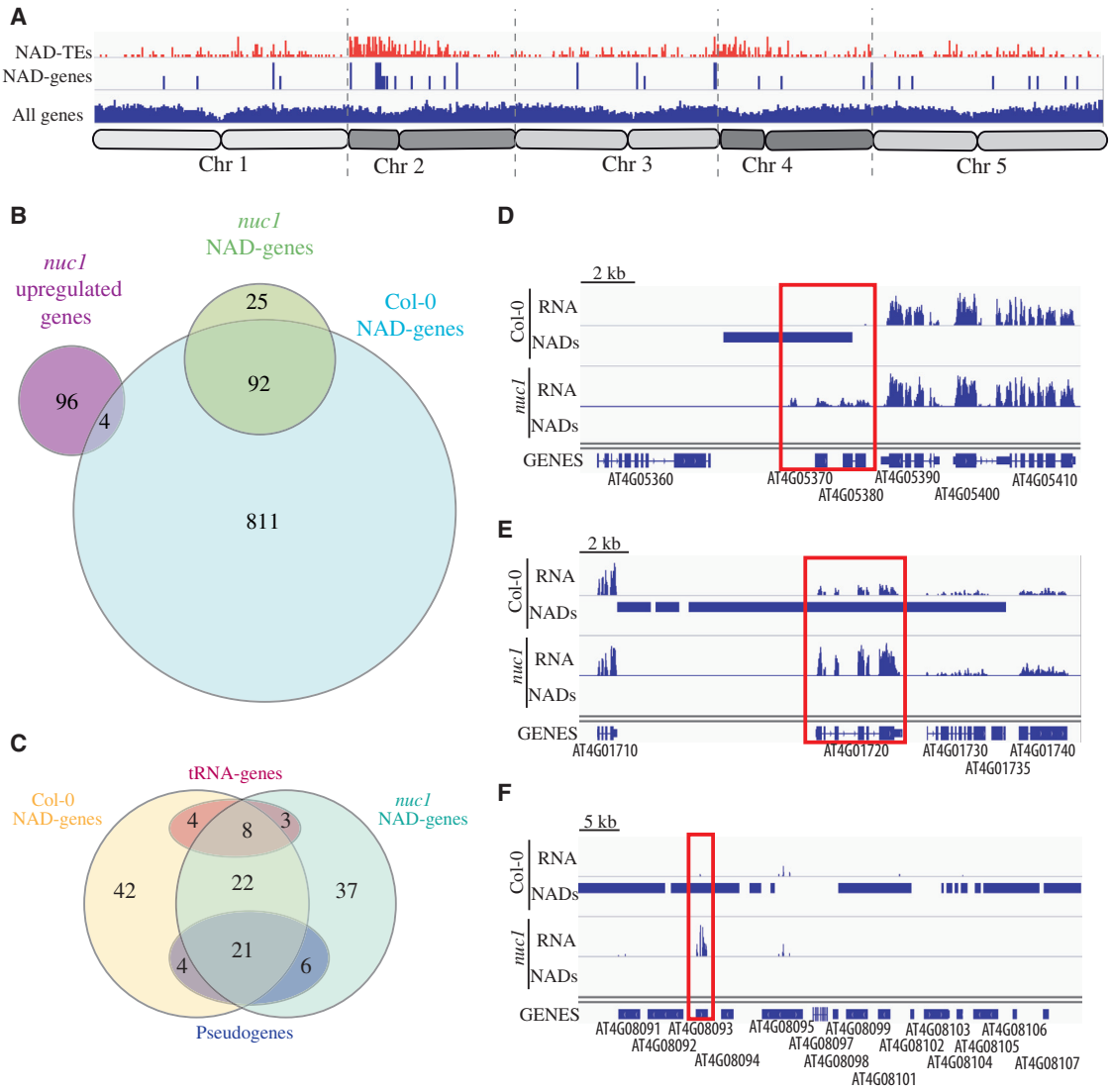

Figure 5. Comparison of NAD Genes in the Wild-Type versus the *nuc1* Mutant

(A) Distribution of all genes, NAD TEs (red), and NAD genes (blue) in the *nuc1* mutant along all five chromosomes.

(B) Venn diagram showing the relation between NAD genes from wild-type Col-0 and the *nuc1* mutant as well as the genes upregulated in the *nuc1* mutant.

(C) Venn diagram displaying common features between NAD genes highly associating with the nucleolus in the wild-type versus the *nuc1* mutant.

(D–F) Genome browser screenshot showing three examples of NAD genes in Col-0 in which nucleolus association is lost in *nuc1* and that are accompanied by a significant increase in their expression.

upregulated genes, four are NAD genes in the wild-type but not in the *nuc1* mutant. Three of these four genes, which are all on chromosome 4, are shown in Figures 5D–5F; they encode for a P loop nucleoside triphosphate hydrolase (AT4G05380), a WRKY transcription factor (AT4G01720), and a pseudogene (AT4G08093), respectively. Note that only genes considered upregulated in *nuc1* by the software Cuffdiff were taken into consideration here. However, more transcripts can be detected in the same region of Chr4S, where nucleolar association in *nuc1* is weaker than in the wild-type (Figure S4). These observations reinforce a possible link between gene activity and nucleolus association.

Nucleolar Clustering of Telomeres Is Disrupted in the *nuc1* Mutant

In *nuc1* mutants, nucleolar organization is disrupted (Pontvianne et al., 2007). Because previous studies have shown that *Arabidopsis* telomeres cluster at the periphery of the nucleolus (Armstrong et al., 2001; Fransz et al., 2002), nucleolar disruption in *nuc1* might alter telomere positioning, potentially influencing the association of linked chromosomal loci with the nucleolus. In the global distribution of NADs along all five chromosomes (Figure 1E), a convex pattern is observed, meaning that sub-telomeric regions are largely enriched in the nucleolus. Interestingly, the sub-telomeric nucleolar association is lower in the

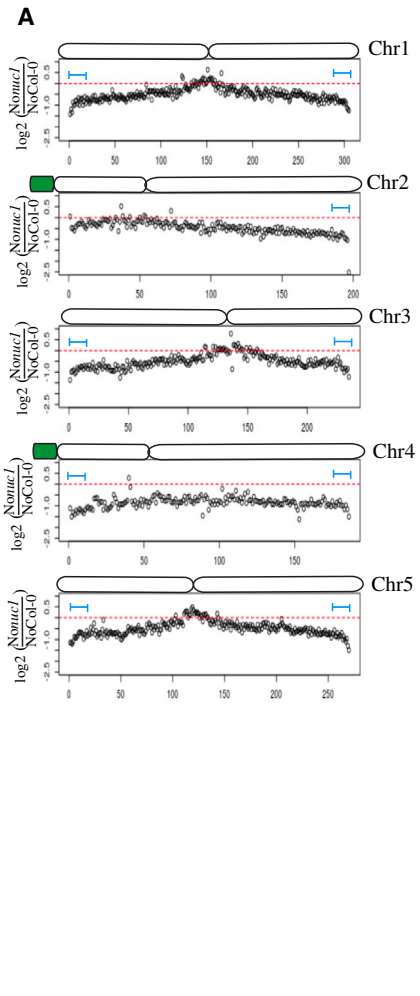

Figure 6. Telomere Nucleolar Clustering Is Affected in the *nuc1* Mutant

(A) Chromosome plot displaying the relative enrichment of the genomic sequence as 100-kb windows in the nucleolus on each five chromosomes of the *nuc1* mutant versus WT Col-0.

(B and C) DNA FISH analyses using a telomere-specific probe (red signal) on DAPI-stained nuclei (blue) from WT Col-0 (B) or *nuc1* plants (C).

(D) Box plot showing the proportion of nucleolus-associated telomeres in WT Col-0 (from 62 nuclei) and the *nuc1* mutant (from 68 nuclei). The asterisk indicates that the enrichment is statistically demonstrated.

nuc1 mutant compared with wild-type Col-0, especially for chromosomes 1, 3, and 5 (Figure 4B). This observation is confirmed by analysis of the relative enrichment in the nucleolus of genomic regions in the *nuc1* mutant compared with wild-type Col-0 (Figure 6A). The latter distribution pattern is concave, demonstrating the enrichment of the centromeric and pericentromeric regions as NADs, but also the depletion of sub-telomeric regions, in the *nuc1* mutant.

The deep sequencing data strongly suggest that nucleolar clustering of telomeres is affected in the *nuc1* mutant. To test this hypothesis with a different method, we conducted DNA FISH analyses of the telomere distribution in wild-type Col-0 and *nuc1* leaf nuclei by using telomere-specific probes (Figures 6B–6D; Figure S5). As expected, FISH signals tend to associate with the nucleolus in wild-type Col-0 nuclei (Figure 6B). However, a significant decrease in telomere association with the nucleolus is observed in the *nuc1* mutant (Figure 6C), with quantification revealing an 83% telomere-nucleolus association in wild-type Col-0 versus 53% in the *nuc1* mutant (Figure 6D). Importantly, telomeres that do not associate with the nucleolus in *nuc1* do not appear to be clustered in an alternative nucleoplasmic subcompartment.

Mutations in *NUC1* Cause Telomere Shortening on All Chromosome Arms

The biological function of telomere nucleolar clustering remains unknown, but we reasoned that it could have an effect on telomere maintenance. The analysis of terminal chromosome restriction fragments (TRFs) allows one to determine global telomere size. We used this technique to determine telomere size distributions in wild-type Col-0 and *nuc1* mutants. In addition, telomere size was analyzed in a mutant for the *NUC2* gene, which encodes another nucleolin-like protein whose function differs from NUC1 (Durut et al., 2014). In addition, telomere size was analyzed in mutants for genes encoding FASCIATA1 (*fas1-4*) and FASCIATA2 (*fas2-4*), which mediate replication-dependent histone deposition and whose disruption strongly reduces telomere size (Mozgová et al., 2010). Compared with wild-type Col-0, a significant TRF length reduction was observed in both *nuc1* mutant alleles, comparable with that observed in *fas1* and *fas2* mutants (Figure 7A). However, no difference is observed between wild-type Col-0, the *nuc2* mutant, or the complemented *nuc2* mutant, demonstrating the specific effect of the *nuc1* mutations.

We previously demonstrated the importance of NUC1 on rRNA gene regulation, which occurs in *NOR2* and *NOR4* (Pontvianne et al., 2010, 2007). In *A. thaliana*, the terminal rRNA genes from *NOR2* and *NOR4* are directly capped by telomere repeats (Copenhaver and Pikaard, 1996). To determine whether telomeres of NOR-bearing chromosomes are differentially affected, we used a PCR-based method called primer extension telomere repeat amplification (PETRA) (Heacock et al., 2004) on multiple chromosome arms (Figures 7B–7E). In agreement with the data from TRF, telomeres on all studied chromosome arms display an ~30% loss of length in the *nuc1* mutants compared with wild-type Col-0, which is equivalent to the loss observed in *fas1* and *fas2* mutants. Together, these observations demonstrate that telomeres from all chromosome arms are shortened

in *nuc1* and thus are not dependent on the presence of rRNA genes near the affected telomere.

The fact that telomeres tend to associate less frequently with the nucleolus and are shorter in *nuc1* mutants compared with the wild-type indicates that NUC1 is somehow important for telomere biology. It remains unknown if these effects are due to *NUC1* disruption, nucleolus disorganization, or both. To test whether NUC1 interacts directly or indirectly with the telomerase, a telomere repeat amplification protocol (TRAP) was performed using immunoprecipitated NUC1 (Figure 7F). Immunoprecipitation (IP) was performed using an anti-FLAG antibody and protein extracts of WT Col-0 or *nuc1* mutant complemented with a transgene encoding NUC1 fused to a FLAG epitope tag under the control of its own promoter (NUC1-FLAG) (Pontvianne et al., 2010). Telomerase activity is markedly stronger in the NUC1-FLAG coIP sample (Figure 7F, left, FLAG-IP) compared with the background signal observed in the Col-0 plant. These data suggest that NUC1 interacts with and coIPs telomerase activity, suggesting a role of NUC1 in telomere biology.

DISCUSSION

The Effect of NOR-Nucleolus Associations on Nuclear Architecture

In mammalian cells, the nuclear distribution of DNA is governed by individual chromosome territories (Gibcus and Dekker, 2013). Although chromosome territories can be seen in *A. thaliana* cells, their distribution in the nucleus is stochastic, with the exception of NOR-bearing chromosomes 2 and 4 (Pecinka et al., 2004). *NOR4*, composed of rRNA gene variants *VAR2* and *VAR3*, associates with the nucleolus (Pontvianne et al., 2013). We demonstrate here that *NOR4* and the entirety of Chr4S, including centromeric and pericentromeric regions, associates with the nucleolus. Consequently, this entire region represents a specific territory or subnuclear compartment. Interestingly, data obtained by chromosome conformation capture indicate that this region acts as an interaction insulator (Feng et al., 2014; Grob et al., 2013). Our results suggest that nucleolus association may be the basis for this insulation.

Coincident with *NOR2* rRNA gene expression in certain mutant backgrounds, the *NOR2* genomic region becomes associated with the nucleolus. Failure to silence *NOR2* rRNA genes occurs in mutants for genes encoding factors implicated in rRNA gene dosage control, such as mutants for histone modifiers (Earley et al., 2010; Pontvianne et al., 2012) as well as *nuc1* (Pontvianne et al., 2007, 2010). As observed for *NOR4* in wild-type Col-0, *NOR2* rRNA gene expression correlates with its nucleolar association but also the nucleolar association of Chr2S, including its centromeric and pericentromeric region. Whether *NOR2* rRNA gene nucleolar association leads to this change in nuclear organization or whether NUC1 influences this organization remains to be tested.

Although Chr4S and/or Chr2S associate with the nucleolus under certain conditions, not all genes present in these genomic regions are necessarily associated with the nucleolus. Loops emanating from Chr4S and oriented within the interior of the nucleus probably exist, allowing actively expressed genes to access a nearby nuclear environment compatible with active gene expression, as described previously (Feng et al., 2014; Fransz et al., 2002).

Pol II-Transcribed Genes Are Present in NADs

Our data have allowed the comprehensive identification of genetic loci that associate with the nucleolus (NADs), including many genes (NAD genes). The majority of NADs correspond to repeat elements such as TEs that are transcriptionally silenced by repressive histone modifications and DNA methylation (Ito and Kakutani, 2014). Whether the association of these loci with the nucleolus participates in transcriptional repression is an open question. However, because only a fraction of TEs associate with the nucleolus, being in a NAD is certainly not a prerequisite for silencing. Our data also demonstrate the presence of genes other than TEs in NADs. In the human nucleolus-associated genome, genes encoding for olfactory receptors or transcription factors were found to be enriched in NAD genes (Németh et al., 2010; van Koningsbruggen et al., 2010). In our data, the most enriched non-rRNA gene loci are pseudogenes. Because they potentially encode truncated or non-functional proteins, keeping them silent is perhaps the best way to prevent a potential deleterious effect of their expression. Importantly, pseudogenes remain highly enriched in the nucleolus of *nuc1* mutant cells, although nucleolar structure is greatly disrupted (Figure 5).

Genes encoding pre-tRNAs are also significantly enriched in the nucleolus. Although this association has never been described in plant cells, previous reports showed a nucleolar association of tRNA genes in yeast and human cells (Németh et al., 2010; Thompson et al., 2003). Interestingly, the presence of a nearby tRNA gene was shown to antagonize pol II RNA transcription in yeast because of its clustering near or in the nucleolus (Wang et al., 2005). This phenomenon is known as tRNA gene-mediated silencing and involves the proteins MOD5 and Condensin (Haeusler et al., 2008; Pratt-Hyatt et al., 2013). However, we show here that several hundred functional genes associate with NADs, and only a small portion have a tRNA gene nearby. Other mechanisms to explain tRNA gene nucleolar association may exist. Whether their association with the nucleolus is biologically relevant remains unknown, but because RNA pol II is depleted in the nucleolus, sequestration of genes to NADs likely reflects a chromatin status or location not conducive to pol II transcription. This hypothesis is reinforced by the observation that NAD genes are typically silent or expressed at low levels but also by the fact that some genes that were NAD genes in Col-0, but not in *nuc1*, became significantly upregulated in *nuc1* (Figure 5). These observations reinforce a possible link between gene silencing and nucleolus association.

Regulation by nucleolar sequestration is known to control certain protein functions, especially during stress conditions. In mammalian cells, rDNA intergenic transcripts accumulate in the nucleolus after heat shock and provoke the nucleolar sequestration of nuclear proteins like the DNA methyltransferase DNMT1, the proteasome factor SUG1, or POLD1, a key factor of DNA replication (Audas et al., 2012a, 2012b). A similar mechanism may exist to regulate transcription by a phenomenon that could be named transcriptional regulation by nucleolar sequestration.

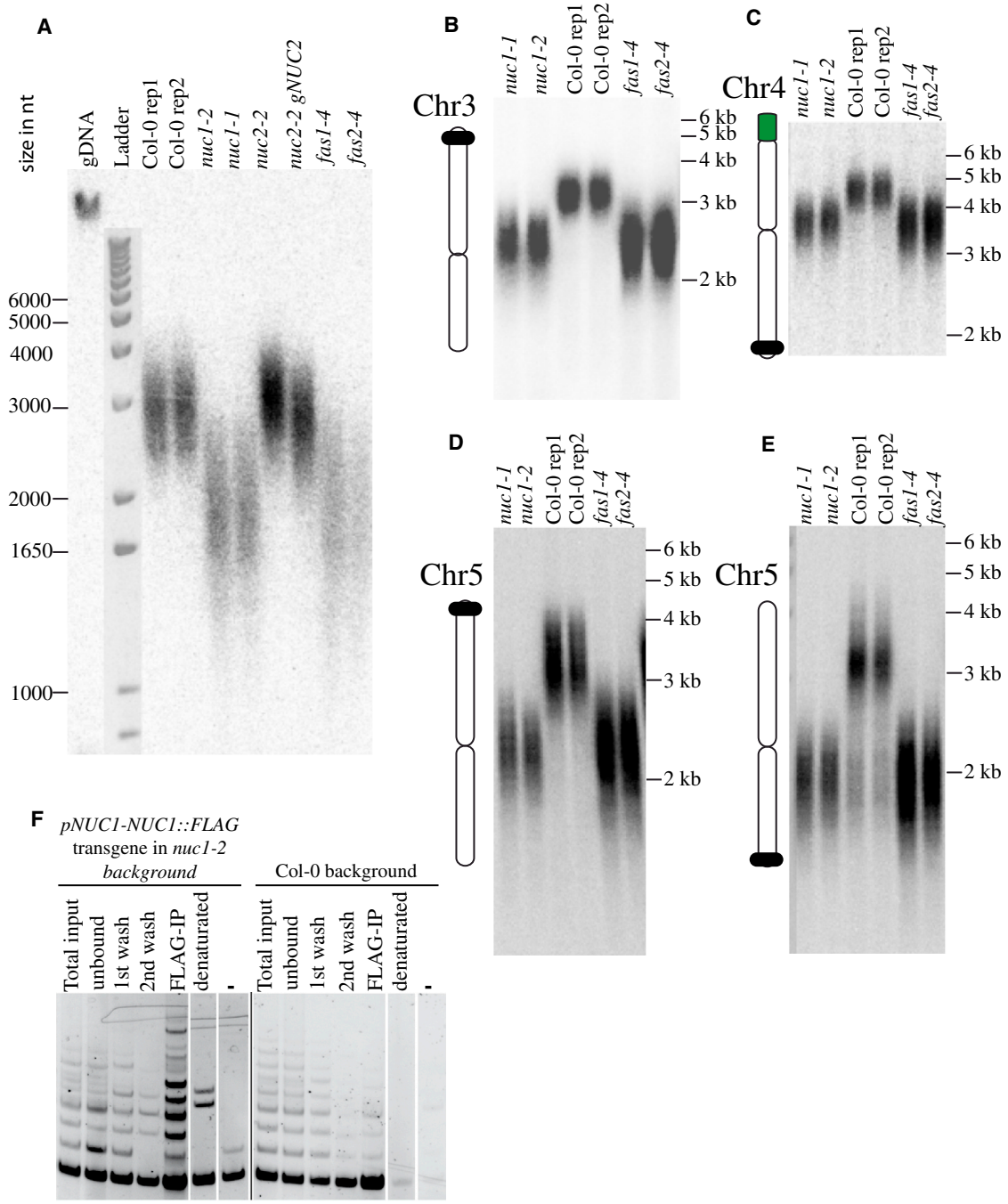

Figure 7. NUC1 Interacts with Telomerase, and Its Disruption Induces Telomere Shortening

(A) TRF analyses of telomere length in two WT Col-0 replicates, two *nuc1* mutant alleles, the *nuc2-2* or complemented *nuc2* mutant, as well as in the *fas1-4* and *fas2-4* mutant.

(B–E) PETRA analyses of telomere length in two *nuc1* mutant alleles, two replicates of WT Col-0, as well as in *fas1-4* and *fas2-4* mutants. Chromosome-specific probes were used to detect the telomere of the left arm of chromosome 3 (B), the right arm of chromosome 4 (C), as well as the left (D) or right (E) arm of chromosome 5.

(F) Telomerase activity was analyzed in fractions obtained during the IP-TRAP experiment using pNUC1-NUC1-FLAG-tagged and WT Col-0 plants. Total input, total protein extract prior to IP; unbound, unbound faction after the capture by ANTI-FLAG magnetic beads; 1st wash, first wash of the fraction bound to magnetic beads with buffer W; 2nd wash, second wash of the fraction bound to magnetic beads with buffer W; FLAG-IP, a fraction specifically bound to magnetic beads; denatured, reaction with denatured total protein extract (5 min, 95°C); −, reaction with buffer W.

Telomere Maintenance and/or Protection Require Their Physical Association with the Nucleolus

In *A. thaliana*, telomeres tend to associate with the nucleolus (Armstrong et al., 2001; Fransz et al., 2002; Roberts et al., 2009). Consequently, we expect subtelomeric regions to be near the nucleolus, as shown previously by DNA FISH (Schubert et al., 2012). Our data demonstrate that at least 100 kb of each region flanking the telomeres strongly associate with the nucleolus. This association may have an effect on genes present in these regions. 39% of highly enriched NAD genes in Col-0 (No/N > 3) are distributed in these subtelomeric regions, whereas they represent less than 1% of the genome. The biological function of telomere nucleolar clustering remains unknown, but some studies have indicated a link between telomere biology and the nucleolus (reviewed in Dvořáčková et al., 2015; Pederson, 1998; Schubert et al., 2014)). In human cells, the telomerase reverse transcriptase (TERT), which catalyzes reverse transcription of the telomerase RNA template into telomeric repeats, is activated in the nucleolus during S phase (Jády et al., 2006; Lee et al., 2014; Tomlinson et al., 2006). In *A. thaliana*, a preferential nucleolar accumulation of telomere repeat-binding (TRB) MYB-like proteins was shown (Dvorácková et al., 2010). In addition, the telomerase RNA-binding protein dyskerin, AtNAP57/CBF5, and AtTERT accumulate in the plant nucleolus (Kannan et al., 2008; Lermontova et al., 2007).

NAD identification in the *nuc1* mutant revealed a decrease in telomere-nucleolus association. At the same time, we demonstrate that telomeres are shortened in the *nuc1* mutant. Previous work demonstrated the important role of nucleolin in rRNA organization and biogenesis (reviewed in Durut and Sáez-Vásquez, 2015)). However, all telomeres are affected in *nuc1,* so the proximity of rRNA genes on a NOR-bearing chromosome cannot explain telomere shortening. Subnucleolar structures show profound changes in *nuc1* mutants, such as the loss of fibrillar centers (FCs), reductions in the dense fibrillar component (DFC), as well as an alteration of the granular component (GC) (Pontvianne et al., 2007). FCs, DFCs, and GCs are subnucleolar structures that are conserved in most eukaryotes and that reflect various steps of ribosome biogenesis (reviewed in Stępiński, 2014; Thiry and Lafontaine, 2005). The nucleolar disorganization observed in *nuc1* mutants reflects the effect of these mutations on rRNA gene regulation. But *nuc1* mutants also affect non-ribosomal nucleolar functions. CoIP TRAP experiments indeed argue in favor of a direct role of NUC1 in telomere biology. Whether NUC1 interacts directly or indirectly with the telomerase holoenzyme will have to be demonstrated by additional experiments. In addition, we cannot conclude whether telomere shortening is a cause or a consequence of telomere mislocalization. However, telomere clustering is not specific to *A. thaliana*. In budding yeast, telomeres cluster in foci at the nuclear periphery in cycling cells (Meister and Taddei, 2013). In quiescent cells, a lack of carbon source is followed by telomeres clustering into a unique focus in the center of the nucleus (Guidi et al., 2015). Although we do not have direct evidence to show it, these data argue in favor of a model where telomere shortening is a consequence of telomere mislocalization, probably because of the absence of NUC1. Combined with previous studies, our work strongly suggests a role for the nucleolus in the biology of telomeres.

EXPERIMENTAL PROCEDURES

Plant Materials and Growth Conditions

Seeds corresponding to the *nuc1-1* and *nuc1-2* (referenced to as *nuc1* throughout the manuscript) plants lines (SALK_053590 and SALK_002764, respectively) were reported previously reported(Pontvianne et al., 2007, 2010) and are available through the Nottingham *Arabidopsis* Stock Centre (NASC). Seeds of the *nuc2-2* mutant (SALK GABI_178D01) and *nuc2*:NUC2 complemented line were described in Durut et al. (2014). Third generations of the knockout mutants *fas1-4* (SAIL_662_D10) and *fas2-4* (SALK_033228) are used in Figure 7 and were described in Exner et al. (2006). For FANoS, wild-type Col-0 expressing the FIB2:YFP fusion protein was described in Pontvianne et al. (2013). The *nuc1-2* plants were crossed with Col-0 FIB2:YFP to introgress the nucleolar marker in the *nuc1-2* mutant background. All plant material used here was grown in control growth chambers on soil at 21°C with a daylight period of 16 hr/day.

Nuclear and Nucleolar DNA Preparation and Sequencing

1 g of leaves from 3-week-old FIB2:YFP plants were fixed for 20 min in 4% formaldehyde in Tris buffer (10 mM Tris-HCl [pH 7.5], 10 mM EDTA, and 100 mM NaCl) and washed twice for 10 min in ice-cold Tris buffer. Washed leaves were minced with a razor blade in 1 ml of 45 mM MgCl2, 20 mM 3-(N-morpholino)propanesulfonic acid (MOPS; pH 7.0), 30 mM sodium citrate, and 0.1% Triton X-100. The homogenate was filtered through 30-μm mesh (PARTEC CellTrics) and subjected to FACS to sort nuclei or sonicated using a Bioruptor (three 5-min pulses, medium power; Diagenode) to liberate nucleoli that were then sorted by FANoS. Sorting of nuclei or nucleoli was triggered by the FIB2:YFP signal using a BD FACS Aria II. Sorted nuclei or nucleoli were treated with RNase A and proteinase K prior to purification and concentration using the ChIP DNA Clean & Concentrator kit (Zymo Research). DNA libraries were generated via the Nextera XT DNA sample preparation kit (Illumina) according to the manufacturer's instructions and were then subjected to high-throughput paired-end 2 × 125 nt sequencing on a Hiseq 2500 apparatus (Illumina). Around 40 million clusters were recovered from the sequencing for each sample.

Cytogenetic Analyses

DNA FISH and DAPI-stained nucleus analyses were performed using nuclei from leaves of 3- or 4-week-old plants as described previously (Pontvianne et al., 2012). The 45S rRNA gene probe was generated by PCR on total genomic DNA from the Col-0 wild-type and corresponds to the region flanking the 45S rRNA gene transcription initiation site (from −223 to +243). The telomere-specific probe was generated by PCR on total genomic DNA from the Col-0 wild-type with the primers 5Telo (TTTAGGGTTTAGGGTTTAGGGTTTAGGGTTTAGGG) and 3Telo (CCCTAAACCCTAAACCCTAAACCCTAAACCCTAAA) prior to its labeling with digoxigenin-11-UTP (Roche). Immunolocalization experiments were performed as described previously (Durut et al., 2014) using the antibody anti-cenH3 (HTR12 NBP1-18694, Novus Biologicals).

Evaluation of Telomere Lengths using TRF and PETRA Analyses

Nucleon Phytopure genomic DNA extraction kits (Illustra) were used for DNA extraction according to the manufacturer's protocol from 3-week-old rosette leaves. 500 ng of genomic DNA was analyzed either by TRF analysis or PETRA. The TRF analysis was performed according to Růcková et al. (2008), and samples were digested by MseI (New England Biolabs). For the PETRA method (Vespa et al., 2007), chromosome-specific primers for 3L, 4R, 5L, and 5R, described in Heacock et al. (2004), were used. Samples from both types of analysis were then separated by 0.8% agarose gel electrophoresis, followed by Southern hybridization with the [32P]-labeled telomeric probe TR4C (CCCTAAA)4.

IP-TRAP

For IP-TRAP, see the Supplemental Experimental Procedures.

Bioinformatic and Statistical Analyses

For each library, 30–50 million reads were obtained, with 85%–90% of the bases displaying a Q score of ≥ 30, with a mean Q score of 38, as assessed with

Fastqc. Thereafter, filtering out of reads corresponding to chloroplastic, mitochondrial, and rRNA genes was performed with bowtie2 (Langmead and Salzberg, 2012). The remaining reads were mapped against the TAIR 10_genome with bowtie2 in sensitive local mode and no mismatch. TEs were analyzed according to the annotation published in Flutre et al. (2011). Quantification by 100-kb windows was made with bedtools software (http://bedtools.readthedocs.org/en/latest/). Regions with a fold change No/N superior to 2 are tagged "differentially covered" (DC). The data are presented in Data S5.

Total RNA was extracted from three pools of 3-week-old *Arabidopsis* plant leaf tissues of wild-type Col-0 or *nuc1* mutant using TRIzol reagent (MRC). Sequencing was performed by the Montpellier GenomiX (MGX) facility (Montpellier) using a Hiseq 2000 to generate 1 × 51-bp-long reads. Illumina reads from non-stranded, polyA+ RNA deep sequencing libraries were aligned to the *A. thaliana* TAIR10-annotated genome reference using Tophat2, Cufflinks, Cuffmerge, and Cuffdiff (Langmead and Salzberg, 2012).

The Z test calculation for two population proportions was used to determine whether the data differ between wild-type Col-0 and the *nuc1* mutant in Figures 2A, 3D, 4E, and 6D.

ACCESSION NUMBERS

The accession numbers for the DNA-seq and RNA-seq data reported in this paper are NCBI: SUB1340932 and BioProject: PRJNA312431, respectively.

SUPPLEMENTAL INFORMATION

Supplemental Information includes Supplemental Experimental Procedures, five figures, and five data files and can be found with this article online at http://dx.doi.org/10.1016/j.celrep.2016.07.016.

AUTHOR CONTRIBUTIONS

M.C. performed most bioinformatic analyses. N.D. and V.P. realized the telomere shortening analyses shown in Figure 7. K.J., S.S., and M.F. realized and analyzed the IP-TRAP assay shown in Figure 7. H.P. and M.R. realized the deep sequencing. C.S.P., J.F., and J.S.V. contributed to the design and/or the interpretation of the data. F.P. designed, performed, and analyzed all experiments except that shown in Figure 7 and wrote the manuscript.

ACKNOWLEDGMENTS

The authors are grateful to Eric Lasserre for help with TE analyses, Pascale Comella for logistic support, Claire Picart for help with confocal microscopy, Todd Blevins for correcting English, and Marie Mirouze for fruitful discussions. We also thank the flow cytometry facility of Montpellier RIO Imaging. This work was supported by CNRS, ANR JCJC NucleoReg (ANR-15-CE12-0013-01) and by BQR2014 (UPVD) LANoS (to F.P.), ANR SubCellif (SVSE2_SUBCELIF 087217) (to J.S.), and GAČR 16-01137S (to J.F.). The international collaboration between France and the Czech Republic is supported by the Barrande program (to J.S. [35626NL] and J.F. [7AMB16FR014]). This work was initially supported by NIH Grant GM60380 (to C.S.P.). C.S.P. is an Investigator of the Howard Hughes Medical Institute and the Gordon and Betty Moore Foundation. The international collaboration between the laboratories of C.S.P. and J.F. is funded by the Ministry of Education, Youth, and Sports of the Czech Republic under the project CEITEC 2020 (LQ1601) and KONTAKT II (LH15189).

Received: February 18, 2016
Revised: May 24, 2016
Accepted: July 3, 2016
Published: July 28, 2016

REFERENCES

Armstrong, S.J., Franklin, F.C., and Jones, G.H. (2001). Nucleolus-associated telomere clustering and pairing precede meiotic chromosome synapsis in Arabidopsis thaliana. J. Cell Sci. *114*, 4207–4217.

Audas, T.E., Jacob, M.D., and Lee, S. (2012a). The nucleolar detention pathway: A cellular strategy for regulating molecular networks. Cell Cycle *11*, 2059–2062.

Audas, T.E., Jacob, M.D., and Lee, S. (2012b). Immobilization of proteins in the nucleolus by ribosomal intergenic spacer noncoding RNA. Mol. Cell *45*, 147–157.

Benoit, M., Layat, E., Tourmente, S., and Probst, A.V. (2013). Heterochromatin dynamics during developmental transitions in Arabidopsis - a focus on ribosomal DNA loci. Gene *526*, 39–45.

Bickmore, W.A., and van Steensel, B. (2013). Genome architecture: domain organization of interphase chromosomes. Cell *152*, 1270–1284.

Boisvert, F.-M., van Koningsbruggen, S., Navascués, J., and Lamond, A.I. (2007). The multifunctional nucleolus. Nat. Rev. Mol. Cell Biol. *8*, 574–585.

Boulon, S., Westman, B.J., Hutten, S., Boisvert, F.-M., and Lamond, A.I. (2010). The nucleolus under stress. Mol. Cell *40*, 216–227.

Chandrasekhara, C., Mohannath, G., Blevins, T., Pontvianne, F., and Pikaard, C.S. (2016). Chromosome-specific NOR inactivation explains selective rRNA gene silencing and dosage control in Arabidopsis. Genes Dev. *30*, 177–190.

Copenhaver, G.P., and Pikaard, C.S. (1996). RFLP and physical mapping with an rDNA-specific endonuclease reveals that nucleolus organizer regions of Arabidopsis thaliana adjoin the telomeres on chromosomes 2 and 4. Plant J. *9*, 259–272.

Dittmer, T.A., Stacey, N.J., Sugimoto-Shirasu, K., and Richards, E.J. (2007). LITTLE NUCLEI genes affecting nuclear morphology in Arabidopsis thaliana. Plant Cell *19*, 2793–2803.

Durut, N., and Sáez-Vásquez, J. (2015). Nucleolin: dual roles in rDNA chromatin transcription. Gene *556*, 7–12.

Durut, N., Abou-Ellail, M., Pontvianne, F., Das, S., Kojima, H., Ukai, S., de Bures, A., Comella, P., Nidelet, S., Rialle, S., et al. (2014). A duplicated NUCLEOLIN gene with antagonistic activity is required for chromatin organization of silent 45S rDNA in Arabidopsis. Plant Cell *26*, 1330–1344.

Dvorácková, M., Rossignol, P., Shaw, P.J., Koroleva, O.A., Doonan, J.H., and Fajkus, J. (2010). AtTRB1, a telomeric DNA-binding protein from Arabidopsis, is concentrated in the nucleolus and shows highly dynamic association with chromatin. Plant J. *61*, 637–649.

Dvořáčková, M., Fojtová, M., and Fajkus, J. (2015). Chromatin dynamics of plant telomeres and ribosomal genes. Plant J. *83*, 18–37.

Earley, K.W., Pontvianne, F., Wierzbicki, A.T., Blevins, T., Tucker, S., Costa-Nunes, P., Pontes, O., and Pikaard, C.S. (2010). Mechanisms of HDA6-mediated rRNA gene silencing: suppression of intergenic Pol II transcription and differential effects on maintenance versus siRNA-directed cytosine methylation. Genes Dev. *24*, 1119–1132.

Exner, V., Taranto, P., Schönrock, N., Gruissem, W., and Hennig, L. (2006). Chromatin assembly factor CAF-1 is required for cellular differentiation during plant development. Development *133*, 4163–4172.

Feng, C.-M., Qiu, Y., Van Buskirk, E.K., Yang, E.J., and Chen, M. (2014). Light-regulated gene repositioning in Arabidopsis. Nat. Commun. *5*, 3027.

Filion, G.J., van Bemmel, J.G., Braunschweig, U., Talhout, W., Kind, J., Ward, L.D., Brugman, W., de Castro, I.J., Kerkhoven, R.M., Bussemaker, H.J., and van Steensel, B. (2010). Systematic protein location mapping reveals five principal chromatin types in Drosophila cells. Cell *143*, 212–224.

Flutre, T., Duprat, E., Feuillet, C., and Quesneville, H. (2011). Considering transposable element diversification in de novo annotation approaches. PLoS ONE *6*, e16526.

Fransz, P., De Jong, J.H., Lysak, M., Castiglione, M.R., and Schubert, I. (2002). Interphase chromosomes in Arabidopsis are organized as well defined chromocenters from which euchromatin loops emanate. Proc. Natl. Acad. Sci. USA *99*, 14584–14589.

Gibcus, J.H., and Dekker, J. (2013). The hierarchy of the 3D genome. Mol. Cell *49*, 773–782.

Grob, S., Schmid, M.W., Luedtke, N.W., Wicker, T., and Grossniklaus, U. (2013). Characterization of chromosomal architecture in Arabidopsis by chromosome conformation capture. Genome Biol. *14*, R129.

Grummt, I., and Längst, G. (2013). Epigenetic control of RNA polymerase I transcription in mammalian cells. Biochim. Biophys. Acta *1829*, 393–404.

Guelen, L., Pagie, L., Brasset, E., Meuleman, W., Faza, M.B., Talhout, W., Eussen, B.H., de Klein, A., Wessels, L., de Laat, W., and van Steensel, B. (2008). Domain organization of human chromosomes revealed by mapping of nuclear lamina interactions. Nature *453*, 948–951.

Guidi, M., Ruault, M., Marbouty, M., Loïodice, I., Cournac, A., Billaudeau, C., Hocher, A., Mozziconacci, J., Koszul, R., and Taddei, A. (2015). Spatial reorganization of telomeres in long-lived quiescent cells. Genome Biol. *16*, 206.

Haeusler, R.A., Pratt-Hyatt, M., Good, P.D., Gipson, T.A., and Engelke, D.R. (2008). Clustering of yeast tRNA genes is mediated by specific association of condensin with tRNA gene transcription complexes. Genes Dev. *22*, 2204–2214.

Heacock, M., Spangler, E., Riha, K., Puizina, J., and Shippen, D.E. (2004). Molecular analysis of telomere fusions in Arabidopsis: multiple pathways for chromosome end-joining. EMBO J. *23*, 2304–2313.

Ito, H., and Kakutani, T. (2014). Control of transposable elements in Arabidopsis thaliana. Chromosome Res. *22*, 217–223.

Jády, B.E., Richard, P., Bertrand, E., and Kiss, T. (2006). Cell cycle-dependent recruitment of telomerase RNA and Cajal bodies to human telomeres. Mol. Biol. Cell *17*, 944–954.

Kannan, K., Nelson, A.D.L., and Shippen, D.E. (2008). Dyskerin is a component of the Arabidopsis telomerase RNP required for telomere maintenance. Mol. Cell. Biol. *28*, 2332–2341.

Kharchenko, P.V., Alekseyenko, A.A., Schwartz, Y.B., Minoda, A., Riddle, N.C., Ernst, J., Sabo, P.J., Larschan, E., Gorchakov, A.A., Gu, T., et al. (2011). Comprehensive analysis of the chromatin landscape in Drosophila melanogaster. Nature *471*, 480–485.

Kind, J., Pagie, L., Ortabozkoyun, H., Boyle, S., de Vries, S.S., Janssen, H., Amendola, M., Nolen, L.D., Bickmore, W.A., and van Steensel, B. (2013). Single-cell dynamics of genome-nuclear lamina interactions. Cell *153*, 178–192.

Kind, J., Pagie, L., de Vries, S.S., Nahidiazar, L., Dey, S.S., Bienko, M., Zhan, Y., Lajoie, B., de Graaf, C.A., Amendola, M., et al. (2015). Genome-wide maps of nuclear lamina interactions in single human cells. Cell *163*, 134–147.

Langmead, B., and Salzberg, S.L. (2012). Fast gapped-read alignment with Bowtie 2. Nat. Methods *9*, 357–359.

Lee, J.H., Lee, Y.S., Jeong, S.A., Khadka, P., Roth, J., and Chung, I.K. (2014). Catalytically active telomerase holoenzyme is assembled in the dense fibrillar component of the nucleolus during S phase. Histochem. Cell Biol. *141*, 137–152.

Lermontova, I., Schubert, V., Börnke, F., Macas, J., and Schubert, I. (2007). Arabidopsis CBF5 interacts with the H/ACA snoRNP assembly factor NAF1. Plant Mol. Biol. *65*, 615–626.

McStay, B., and Grummt, I. (2008). The epigenetics of rRNA genes: from molecular to chromosome biology. Annu. Rev. Cell Dev. Biol. *24*, 131–157.

Meister, P., and Taddei, A. (2013). Building silent compartments at the nuclear periphery: a recurrent theme. Curr. Opin. Genet. Dev. *23*, 96–103.

Mozgová, I., Mokros, P., and Fajkus, J. (2010). Dysfunction of chromatin assembly factor 1 induces shortening of telomeres and loss of 45S rDNA in Arabidopsis thaliana. Plant Cell *22*, 2768–2780.

Németh, A., Conesa, A., Santoyo-Lopez, J., Medina, I., Montaner, D., Péterfia, B., Solovei, I., Cremer, T., Dopazo, J., and Längst, G. (2010). Initial genomics of the human nucleolus. PLoS Genet. *6*, e1000889.

Padeken, J., Mendiburo, M.J., Chlamydas, S., Schwarz, H.-J., Kremmer, E., and Heun, P. (2013). The nucleoplasmin homolog NLP mediates centromere clustering and anchoring to the nucleolus. Mol. Cell *50*, 236–249.

Pecinka, A., Schubert, V., Meister, A., Kreth, G., Klatte, M., Lysak, M.A., Fuchs, J., and Schubert, I. (2004). Chromosome territory arrangement and homologous pairing in nuclei of Arabidopsis thaliana are predominantly random except for NOR-bearing chromosomes. Chromosoma *113*, 258–269.

Pederson, T. (1998). The plurifunctional nucleolus. Nucleic Acids Res. *26*, 3871–3876.

Pederson, T. (2011). The nucleolus. Cold Spring Harb. Perspect. Biol. *3*, a000638.

Pontvianne, F., Matía, I., Douet, J., Tourmente, S., Medina, F.J., Echeverria, M., and Sáez-Vásquez, J. (2007). Characterization of AtNUC-L1 reveals a central role of nucleolin in nucleolus organization and silencing of AtNUC-L2 gene in Arabidopsis. Mol. Biol. Cell *18*, 369–379.

Pontvianne, F., Abou-Ellail, M., Douet, J., Comella, P., Matia, I., Chandrasekhara, C., Debures, A., Blevins, T., Cooke, R., Medina, F.J., et al. (2010). Nucleolin is required for DNA methylation state and the expression of rRNA gene variants in Arabidopsis thaliana. PLoS Genet. *6*, e1001225.

Pontvianne, F., Blevins, T., Chandrasekhara, C., Feng, W., Stroud, H., Jacobsen, S.E., Michaels, S.D., and Pikaard, C.S. (2012). Histone methyltransferases regulating rRNA gene dose and dosage control in Arabidopsis. Genes Dev. *26*, 945–957.

Pontvianne, F., Blevins, T., Chandrasekhara, C., Mozgová, I., Hassel, C., Pontes, O.M.F., Tucker, S., Mokros, P., Muchová, V., Fajkus, J., and Pikaard, C.S. (2013). Subnuclear partitioning of rRNA genes between the nucleolus and nucleoplasm reflects alternative epiallelic states. Genes Dev. *27*, 1545–1550.

Pratt-Hyatt, M., Pai, D.A., Haeusler, R.A., Wozniak, G.G., Good, P.D., Miller, E.L., McLeod, I.X., Yates, J.R., 3rd, Hopper, A.K., and Engelke, D.R. (2013). Mod5 protein binds to tRNA gene complexes and affects local transcriptional silencing. Proc. Natl. Acad. Sci. USA *110*, E3081–E3089.

Roberts, N.Y., Osman, K., and Armstrong, S.J. (2009). Telomere distribution and dynamics in somatic and meiotic nuclei of Arabidopsis thaliana. Cytogenet. Genome Res. *124*, 193–201.

Roudier, F., Ahmed, I., Bérard, C., Sarazin, A., Mary-Huard, T., Cortijo, S., Bouyer, D., Caillieux, E., Duvernois-Berthet, E., Al-Shikhley, L., et al. (2011). Integrative epigenomic mapping defines four main chromatin states in Arabidopsis. EMBO J. *30*, 1928–1938.

Roy, S., Ernst, J., Kharchenko, P.V., Kheradpour, P., Negre, N., Eaton, M.L., Landolin, J.M., Bristow, C.A., Ma, L., Lin, M.F., et al.; modENCODE Consortium (2010). Identification of functional elements and regulatory circuits by Drosophila modENCODE. Science *330*, 1787–1797.

Růcková, E., Friml, J., Procházková Schrumpfová, P., and Fajkus, J. (2008). Role of alternative telomere lengthening unmasked in telomerase knock-out mutant plants. Plant Mol. Biol. *66*, 637–646.

Schubert, V., and Weisshart, K. (2015). Abundance and distribution of RNA polymerase II in Arabidopsis interphase nuclei. J. Exp. Bot. *66*, 1687–1698.

Schubert, V., Berr, A., and Meister, A. (2012). Interphase chromatin organisation in Arabidopsis nuclei: constraints versus randomness. Chromosoma *121*, 369–387.

Schubert, V., Rudnik, R., and Schubert, I. (2014). Chromatin associations in Arabidopsis interphase nuclei. Front. Genet. *5*, 389.

Sequeira-Mendes, J., and Gutierrez, C. (2015). Genome architecture: from linear organisation of chromatin to the 3D assembly in the nucleus. Chromosoma.

Sequeira-Mendes, J., Aragüez, I., Peiró, R., Mendez-Giraldez, R., Zhang, X., Jacobsen, S.E., Bastolla, U., and Gutierrez, C. (2014). The Functional Topography of the Arabidopsis Genome Is Organized in a Reduced Number of Linear Motifs of Chromatin States. Plant Cell *26*, 2351–2366.

Stępiński, D. (2014). Functional ultrastructure of the plant nucleolus. Protoplasma *251*, 1285–1306.

Thiry, M., and Lafontaine, D.L.J. (2005). Birth of a nucleolus: the evolution of nucleolar compartments. Trends Cell Biol. *15*, 194–199.

Thompson, M., Haeusler, R.A., Good, P.D., and Engelke, D.R. (2003). Nucleolar clustering of dispersed tRNA genes. Science *302*, 1399–1401.

Tomlinson, R.L., Ziegler, T.D., Supakorndej, T., Terns, R.M., and Terns, M.P. (2006). Cell cycle-regulated trafficking of human telomerase to telomeres. Mol. Biol. Cell *17*, 955–965.

Tucker, S., Vitins, A., and Pikaard, C.S. (2010). Nucleolar dominance and ribosomal RNA gene silencing. Curr. Opin. Cell Biol. *22*, 351–356.

van Koningsbruggen, S., Gierlinski, M., Schofield, P., Martin, D., Barton, G.J., Ariyurek, Y., den Dunnen, J.T., and Lamond, A.I. (2010). High-resolution whole-genome sequencing reveals that specific chromatin domains from most human chromosomes associate with nucleoli. Mol. Biol. Cell *21*, 3735–3748.

Vespa, L., Warrington, R.T., Mokros, P., Siroky, J., and Shippen, D.E. (2007). ATM regulates the length of individual telomere tracts in Arabidopsis. Proc. Natl. Acad. Sci. USA *104*, 18145–18150.

Wang, L., Haeusler, R.A., Good, P.D., Thompson, M., Nagar, S., and Engelke, D.R. (2005). Silencing near tRNA genes requires nucleolar localization. J. Biol. Chem. *280*, 8637–8639.

Wang, Z., Zang, C., Rosenfeld, J.A., Schones, D.E., Barski, A., Cuddapah, S., Cui, K., Roh, T.-Y., Peng, W., Zhang, M.Q., and Zhao, K. (2008). Combinatorial patterns of histone acetylations and methylations in the human genome. Nat. Genet. *40*, 897–903.